ChemComm

FEATURE ARTICLE

View Article Online
View Journal | View Issue

Cite this: *Chem. Commun.*, 2025, **61**, 5871

Advancing metallomimetic catalysis through structural constraints of cationic P^{III} species

Deependra Bawari,* Donia Toami and Roman Dobrovetsky*

In recent years, the concept of structural constraints on the main-group (MG) centers has emerged as a powerful strategy to enhance their reactivity. Among these, structurally constrained (SC) phosphorus centers have garnered significant attention due to their ability to cycle between two stable oxidation states, P(III) and P(V), making them highly promising for small molecule activation and catalysis. Structural constraints grant phosphorus centers transition metal (TM)-like reactivity, enabling the activation of small molecules by these SC P(III) centers, a reactivity previously inaccessible with conventional phosphines or other phosphorus derivatives. This feature article reviews recent advances in the chemistry of cationic, structurally constrained P(III) (CSCP) compounds, emphasizing their ability to mimic TM behavior in small-molecule activation and catalysis, particularly through the key elementary steps of TM-based catalysis, such as oxidative addition (OA), migratory insertion (MI), ligand metathesis (LM), reductive elimination (RE), *etc.* The development of these SC cationic P(III) species highlights the interplay between structural constraints and cationic charge, facilitating analogous metallomimetic reactivity in other main-group elements.

Received 10th February 2025,
Accepted 19th March 2025

DOI: 10.1039/d5cc00723b

rsc.li/chemcomm

1. Introduction

The search for sustainable alternatives to transition-metal (TM) based catalysts has driven scientists to explore main-group (MG) compounds for small-molecule activation and catalysis, making it a vibrant field of research over the past two decades.[1–4] Among MG elements, pnictogens stand out for their ability to switch between two stable oxidation states ($E^n \rightleftharpoons E^{n+2}$; E = P, Sb, Bi), a property that enables them to mimic TMs' chemistry and thus react *via* similar key elementary steps such as oxidative addition (OA) and reductive elimination (RE).[5–12] These properties position pnictogens as emerging players in TM-free redox catalysis.

While most neutral pnictogen species exhibit limited reactivity towards small molecules in their common oxidation states, imposing structural constraints on these molecular centers,[13–19] particularly phosphorus (P), has unlocked their potential for small-molecule activation.[20–24] A common strategy for achieving this involves enclosing pnictogen centres within rigid pincer-type ligands.[20–24] This constraint induces a deviation from typical VSEPR geometries, disrupting the local symmetry around the pnictogen atom (Fig. 1). Consequently, the frontier molecular orbitals rehybridize, and the HOMO–LUMO energy gap decreases, which enhances the ambiphilicity (nucleo- and electrophilicity) of these centers and significantly improves their ability to activate strong chemical bonds.[20–24]

In the past decade, there has been a steady rise in the development of molecules featuring structurally constrained (SC) phosphorus centers. The earliest examples of structurally constrained phosphorus (SCP) species (**I–III**) were reported in the early 1980s by the groups of Houalla,[25–28] Contreras,[29–32] and Baccolini.[33–35] While these pioneering studies primarily focused on the synthesis of phosphorus (P^{III} and P^{V}) derivatives (Fig. 2a), they laid the foundation for exploring the reactivity of modern SCP compounds.

In 1984, Arduengo reported a seminal discovery of an SC, T-shaped phosphorus center (**IV**) in an *ONO*-type pincer ligand

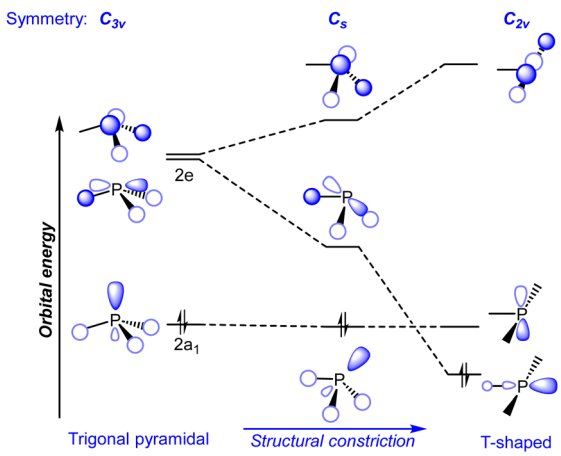

Fig. 1 A qualitative Walsh diagram illustrating the changes in molecular orbital energies and their corresponding shapes as a trigonal pyramidal phosphorus center distorts toward a planar T-shaped geometry.

School of Chemistry, Raymond and Beverly Sackler Faculty of Exact Sciences, Tel Aviv University, Tel Aviv 69978, Israel. E-mail: rdobrove@tau.ac.il, deependrabawari@gmail.com

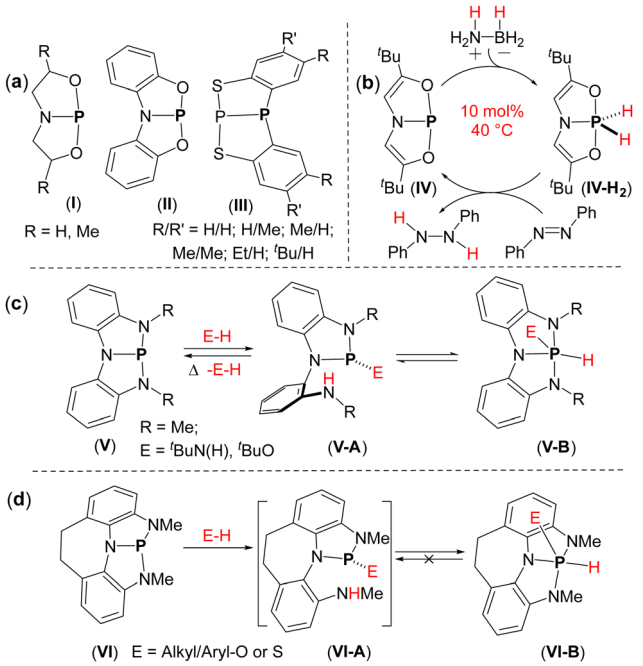

Fig. 2 Known examples of SCPs and their use in the activation of various E–H bonds.

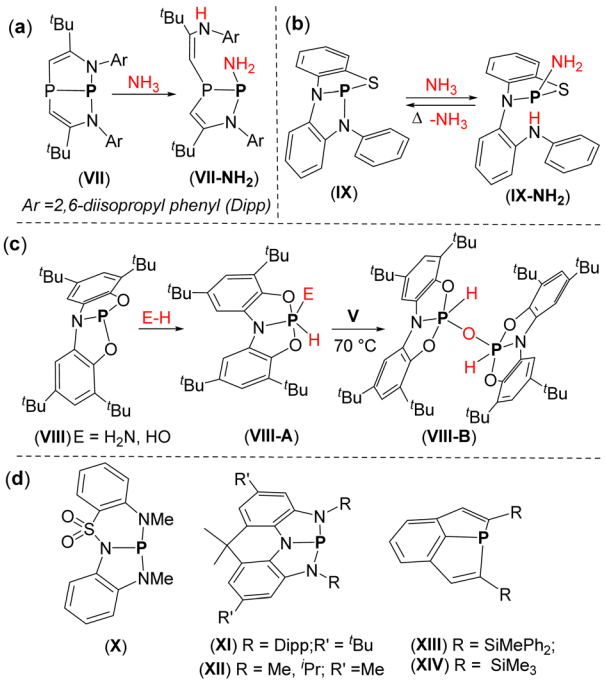

Fig. 3 Known examples of SCPs and their use in the activation of various E–H bonds.

(Fig. 2b), capable of activating O–H bonds in MeOH *via* an OA-type reaction at the P^{III} centre.[36,37] After a period of limited progress, Radosevich and co-workers revived interest in SCPs in 2012 by demonstrating the catalytic transfer hydrogenation of azobenzene using **IV** and H_3NBH_3 as hydrogen source (Fig. 2b).[38]

The same group later showed OA-type reactions of the N–H bonds in NH_3 and alkyl/arylamines at the P^{III} centre in **IV**.[39] Subsequently, Radosevich reported an SCP compound (**V**) in an NNN-type pincer ligand with an aromatic backbone.[40] This SCP species activated the E–H bonds (E = N, O) in NH_3, alkyl/arylamines, carboxylic acids, and alkyl/aryl alcohols (Fig. 2c). Mechanistic studies revealed that the OA step was preceded by E–H bond cleavage through phosphorus-ligand assisted cooperation (LA), followed by intramolecular σ^3-P → σ^5-P tautomerism. Interestingly, a later-reported derivative of **V**, featuring an ethylene-bridged backbone (**VI**), exhibited a preference for the σ^5-P product, despite retaining the same local structure and bonding around the P-center as **V**.[41] This shift was attributed to the restricted rotation of the C_{aryl}–N bond in the σ^3-P product, favouring the σ^5-P isomer (Fig. 2d). Notably, the resulting P^V product, **V-B**, could undergo reductive elimination of anilines and alcohols at elevated temperatures, highlighting its potential for catalytic applications (Fig. 2c).

Additionally, **V** successfully activated the B–H and C–F bonds and was subsequently employed in the hydroboration of imines and the non-catalytic, metallomimetic hydrodefluorination of fluoroarenes, clearly underscoring the significant catalytic potential of these species.[42,43]

Ammonia activation is essential in energy production and synthetic chemistry.[44a,b] While most TMs do not activate NH_3 through formal oxidative addition, but instead form Werner-type complexes,[44c,d] certain MG compounds have demonstrated the potential to activate the N–H bonds in ammonia.[39,45–53] In the case of SCPs, Hirao and Kinjo used an *NPN*-type pincer ligand with an aliphatic backbone to synthesize a diazadiphosphapentalene (**VII**), which effectively activated the H_2N–H bond *via* σ bond metathesis (Fig. 3a).[54] Aldridge and Goicoechea reported the SCP species, **VIII**, featuring an *ONO*-type pincer ligand with an aromatic backbone (Fig. 3c).[55] **VIII** readily activated the N–H bond in NH_3 through oxidative addition (OA) to the P-center (Fig. 3c). Interestingly, the O–H bonds in H_2O were also activated *via* OA to the P-center, with both O–H bonds reacting when two equivalents of **VIII** were used (Fig. 3c).

Noteworthy, all the SCP systems discussed above activated NH_3 irreversibly (Fig. 3a and c) *i.e.*, no reductive elimination of the ammonia regenerating the starting SCP species was observed. The first neutral SCP in an *NNS*-type ligand (**IX**) capable of activating NH_3 and releasing it upon mild heating was reported by Goicoechea and co-workers in 2021 (Fig. 3b).[56] In 2023, Vlugt and co-workers introduced an SCP centre in a non-symmetric *NNN*-type ligand (**X**) that could reversibly activate the N–H bond in dimethylamine (Fig. 3d).[57] Beyond these examples, recent years have seen the emergence of several other intriguing SCP species, including **V** (R = ^{i}Pr, 2-Py, $SiMe_3$)[19,40,58] and **XI–XIV**[59–61] each showcasing unique and fascinating chemistry (Fig. 3d).

2. Cationic, structurally constrained P^{III} species

The field of P^{III} cations began with the synthesis of phosphenium cations in 1964 by Dimroth and Hoffmann,[62] and had been largely dominated by N-heterocyclic phosphenium cations (NHPs).[63,64] While NHPs are isolable, akin to N-heterocyclic

carbenes (NHCs),[65,66] their electronic properties are fundamentally different. Due to their cationic nature, NHPs are weak σ-donors and strong π-acceptors,[67,68] making them highly effective ligands for electron-rich TM complexes.[69–73] In contrast to ambiphilic carbenes,[45,74,75] NHPs exhibit relatively low reactivity toward small molecules. In fact, only a few NHPs have demonstrated the ability to activate bonds in small molecules.[76,77] Non-NHP phosphenium cations, particularly dications, have been shown to activate O–H bonds, but exhibit limited reactivity with Si–H and B–H bonds.[78,79]

As mentioned earlier, the use of rigid scaffolds to constrain phosphorus centers has enabled the activation of E–H bonds (E = B, N, O, S, C–X, where X = N, F, Cl, Br, I) in neutral SCP species.[36–43,54–61,80] The catalytic applications of neutral SCP compounds, however, have been largely limited to species **IV** and **V**. One strategy to further enhance the reactivity of SCP centers is to introduce a cationic charge, preferably localized on the phosphorus atom. This modification is expected to significantly boost reactivity by further lowering the LUMO. Literature precedents demonstrate that the presence of a cationic charge often yields more electrophilic species compared to their neutral counterparts. A notable example is borenium ions, which can catalyze reactions by activating a variety of small molecules.[81] This type of enhanced reactivity is well illustrated by recent examples of cationic SCP species (CSCPs) (**2**, **6**, **11**, **13**, **17**, **24**, and **34**), which demonstrated the ability to activate a broad range of bonds, including O–H, N–H, C–H, C–F, Si–H, and H–H bonds (Fig. 4–13).[82–88]

Notably, in contrast to neutral SCP species, their cationic analogues have also found application in metallomimetic catalysis. For instance, the OA type reaction of the Si–H bond has been employed in the catalytic hydrosiliylation of aldehydes;[86] the OA of C–F bonds has been utilized in catalytic hydrodefluorination and C–N bond cross-coupling reactions;[87] and the OA of the H–H bond has been applied in catalytic hydrogenation.[88]

While the chemistry of neutral SCP species has been periodically reviewed over the years, the field of CSCP species is relatively young and remains less explored. This feature article provides an overview of recent advancements in CSCP chemistry, highlighting key distinctions from neutral SCP compounds in terms of synthetic methods, chemical properties, and potential applications.

Aldridge and Goicoechea reported the reaction of **VIII** with HOTf or MeOTf (OTf = trifluoromethanesulfonate) leading to P^{III} cations, **1A** and **1B** (Fig. 4a).[89] The single crystal X-ray diffraction (SCXRD) structures of **1A** and **1B** revealed a significant distortion around the phosphorus centre and considerable elongation of the N–P bonds (1.92 and 1.95 Å, respectively) compared to the starting SCP compound, **VIII** (1.757(1) Å). However, the chemistry of these cations (**1A** and **1B**) was not investigated.

In 2018, Dobrovetsky and co-workers reported a cationic phosphenium species, **2**, featuring an *ONO* scaffold (**2-L**) with pyridine as the central donor.[82] The synthesis of **2** involved first the preparation of chlorophosphine (**2-Cl**) by reacting PCl_3 with **2-LH$_2$** (Fig. 4b). Notably, **2-Cl** was shown to be solvent dependent, in polar solvents the P–Cl bond dissociated forming the cationic [**2**][Cl]. An anion exchange reaction with weakly coordinating anion $[B(C_6F_5)_4]^-$ resulted in the formation of a ion separated phosphenium cation, [**2**][$B(C_6F_5)_4$]. The SCXRD of [**2**][$B(C_6F_5)_4$] revealed a significant distortion in local symmetry around the P-centre. Noteworthy, the P–N bond length in **2** was significantly shorter (1.81 Å), in comparison to the P–N bond lengths in **1A** and **1B** (1.92 and 1.95 Å, respectively).

The preliminary reactivity of **2** with H_2O and ROH (R = Me, ^{i}Pr, ^{t}Bu, and Ph) was studied. Remarkably, **2** reacted with H_2O and ROH (R = Me, ^{i}Pr, ^{t}Bu) by the OA-type reactions of the O–H bonds to the P-center producing P^V cations, **3a–3d** (Fig. 4c). However, no reaction was observed with phenol, even at elevated temperatures. Additionally, **2** reacted with NH_3 *via*

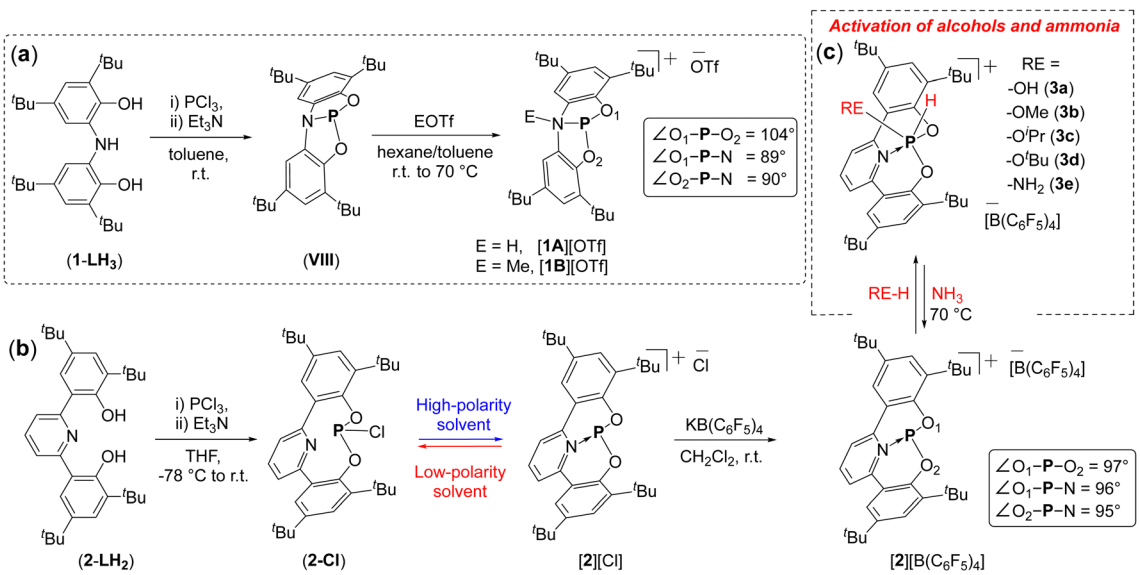

Fig. 4 Synthetic scheme for the synthesis of: (a) [**1A**][OTf] and [**1B**][OTf]; (b) [**2**][$B(C_6F_5)_4$] and the activation of O–H and N–H bonds by **2**.

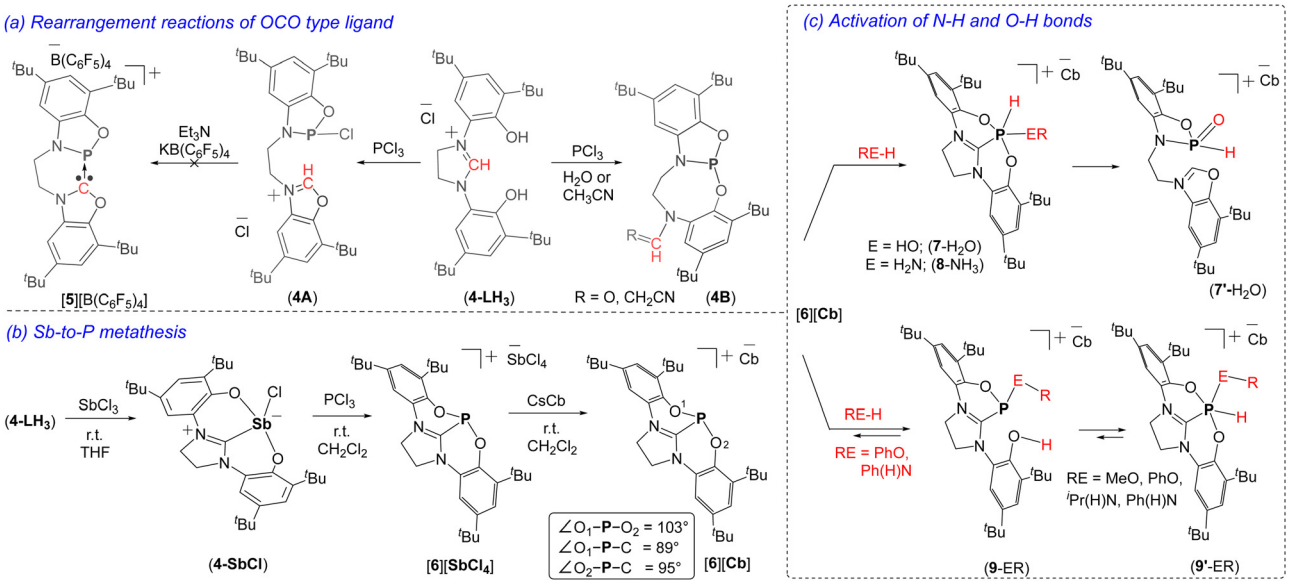

Fig. 5 Synthetic scheme showing: (a) phosphorus mediated rearrangement of an *OCO* type ligand; (b) Sb-to-P metathesis to prepare CSCP, [**6**][$SbCl_4$] and [**6**][Cb]; (c) activation reactions of O–H and N–H bonds by [**6**][Cb].

an OA-type reaction, leading to the formation of a P^V compound (**3e**) which, interestingly, undergoes reductive elimination of NH_3 at 70 °C, regenerating **2**. The reversible nature of NH_3 activation at phosphorus centre was unprecedented at the time and emphasized the novel reactivity derived from the combination of structural constraint and cationic character of the P-centre.

In recent years, dianionic, tridentate pincer-type ligands with NHC central donor have demonstrated significant utility in stabilizing a range of both early and late TM complexes.[90–93] However, their application to MG elements has remained relatively underexplored.[94–96]

Attempts to obtain CSCP species **6** (Fig. 5b) through the reaction of **4-LH$_3$** with PCl_3 led to the rearrangement of imidazolinium to oxazolium ring (**4A**) mediated by the phosphorus centre (Fig. 5a).[97] Interestingly when the reaction is carried out in the presence of H_2O or CH_3CN, different rearrangements lead to the formation of a neutral (**4B**) through a multi-step process, as illustrated in Fig. 5a.[80a] All the attempts to deprotonate **4A** to obtain the CSCP species **5** failed (Fig. 5a). In contrast, the reaction of **4-LH$_3$** with $SbCl_3$ readily leads to the antimony chloride **4-SbCl** (Fig. 5b).[83] While the synthesis of **6** *via* the reaction of deprotonated **4-LH$_3$** with PCl_3 failed, the use of **4-SbCl** as a template for the Sb-to-P metathesis with PCl_3 led directly to the desired [**6**][$SbCl_4$] (Fig. 5b). The SCXRD structure of [**6**][$SbCl_4$] revealed notable distortion around the phosphorus center ($\angle O_1$–P–O_2 = 103°; $\angle O_1$–P–C = 89°; $\angle O_2$–P–C = 95°). Both the molecular structure and density functional theory (DFT) computational analysis of **6** suggested that the formal positive charge is divided between the two nitrogen atoms of the imidazolinium ring.

The reactivity of [**6**][$SbCl_4$] with H_2O and amines showed that $[SbCl_4]^-$ anion is non-innocent in these reactions. Therefore, it was replaced with the carborane anion, $[CB_{11}H_{12}]^-$ (Cb) using CsCb, yielding [**6**][Cb] (Fig. 5b). [**6**][Cb] successfully activated O–H and N–H bonds in H_2O and NH_3 *via* formal OA of the O–H or N–H bonds to the P-center leading to **7-H$_2$O** and **8-NH$_3$** (Fig. 5c). **7-H$_2$O** was not a stable compound under the reaction conditions and rapidly underwent rearrangement of the imidazolinium unit to oxazolium (**7′-H$_2$O**). Unlike the reversible H_2N–H bond activation by **2** (Fig. 4c), **8-NH$_3$** did not exhibit reversible reductive elimination of the NH_3 fragment.

More interesting results were obtained in the reaction of [**6**][Cb] with alcohols and amines. In these cases, the reaction of [**6**][Cb] with MeOH, ^{i}PrNH$_2$, PhOH, and $PhNH_2$ reaches an equilibrium between the LA and OA products. Notably, in the case of PhOH and $PhNH_2$, the LA product undergoes reductive elimination of PhOH and $PhNH_2$ at room temperature, regenerating [**6**][Cb]. DFT calculations supported the thermoneutral nature of these reactions. It is worth noting that unlike **2**, **6** was capable of activation of the PhO–H bond.

While Dobrovetsky and co-workers were unsuccessful in the synthesis of CSCP species **5** (Fig. 5a), Radosevich and Greb recently reported a series of phosphenium cations similar to **5**, **11A–D**, with pyridine-type donors in *NNO* scaffolds (Fig. 6a).[84] The CSCP **11A–D** were synthesized by chloride abstraction from the corresponding chlorophosphines (**10-Cl**) using $NaB(C_6F_5)_4$ or $LiAl(OR^F)_4$ (Fig. 6a). In contrast to the nitrogen-donor-based cationic P^{III} species **1** and **2**, the SCXRD structure of **11A–D** revealed more pronounced distortion, with bond angles $\angle N_1$–P–O = 108°, $\angle N_1$–P–N_2 = 86°, and $\angle N_2$–P–O = 94°.

The low-temperature NMR and DFT calculations of **11A–D** suggested a rapid dynamic conformational process in solution, occurring *via* the isomerization of the bent **11A** structures. This process involves a metastable, T-shaped planar intermediate (**11-IM**; ΔG = 4.1 kcal mol^{-1}) (Fig. 6b). Notably, the calculations also revealed that planarization of the bent global minimum positions the frontier orbitals at the P center, whereas in the bent form, these orbitals reside on the ligands. Additionally,

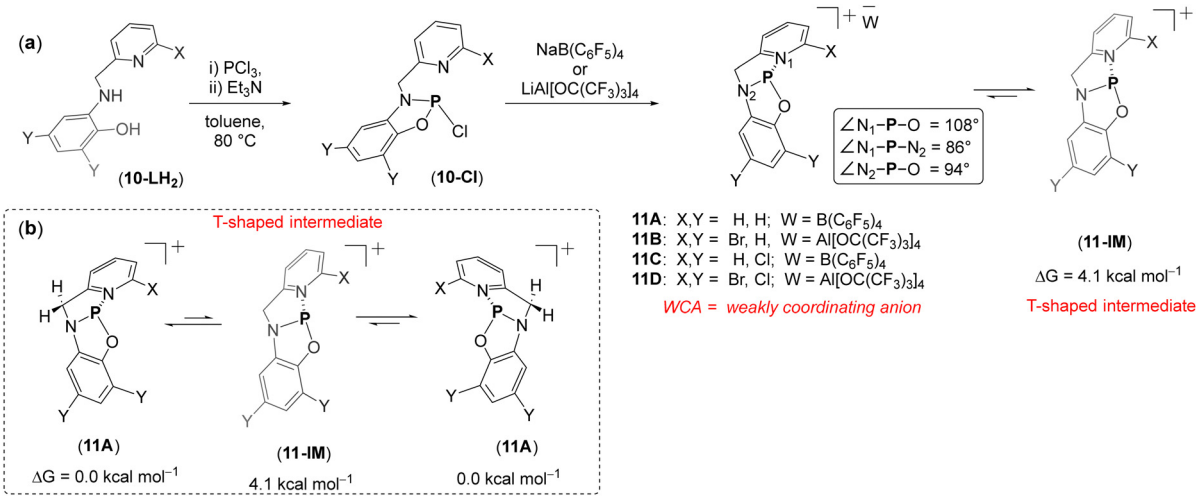

Fig. 6 Synthetic scheme for the synthesis of (a) [**11**][W]; (b) isomerization between bent structures of **11** *via* a T-shaped planar structure.

the planarization significantly lowers the energy of the LUMO orbitals, resulting in a smaller HOMO–LUMO gap (2.5 eV). It was therefore suggested by the authors that the T-shaped intermediate (**11-IM**) is the key intermediate in bond activation reactions.

Remarkably **11A** activates the C–H bonds in 1-methylindole and phenylacetylene at room temperature, producing OA-type products (Fig. 7b). DFT calculations of **11A** with *N*-methylpyrrole as a model substrate revealed that the C–H bond activation proceeds through T-shaped intermediate **11-IM**. Initially, the C–H bond is cleaved between the P- and $N_{pyridine}$ centres through a phosphorus-ligand cooperation mechanism. The resulting species, **11-IM-A**, then isomerizes to **11-IM-B**, which undergoes σ^3-P/σ^5-P tautomerization, transferring the hydrogen from nitrogen to the phosphorus centre and leading to the formation of the C–H activated product **12** (Fig. 7a). Notably, the intermediates (**11-IM-A**) and (**11-IM-B**) were not observed experimentally, suggesting their rapid conversion to the final OA product.

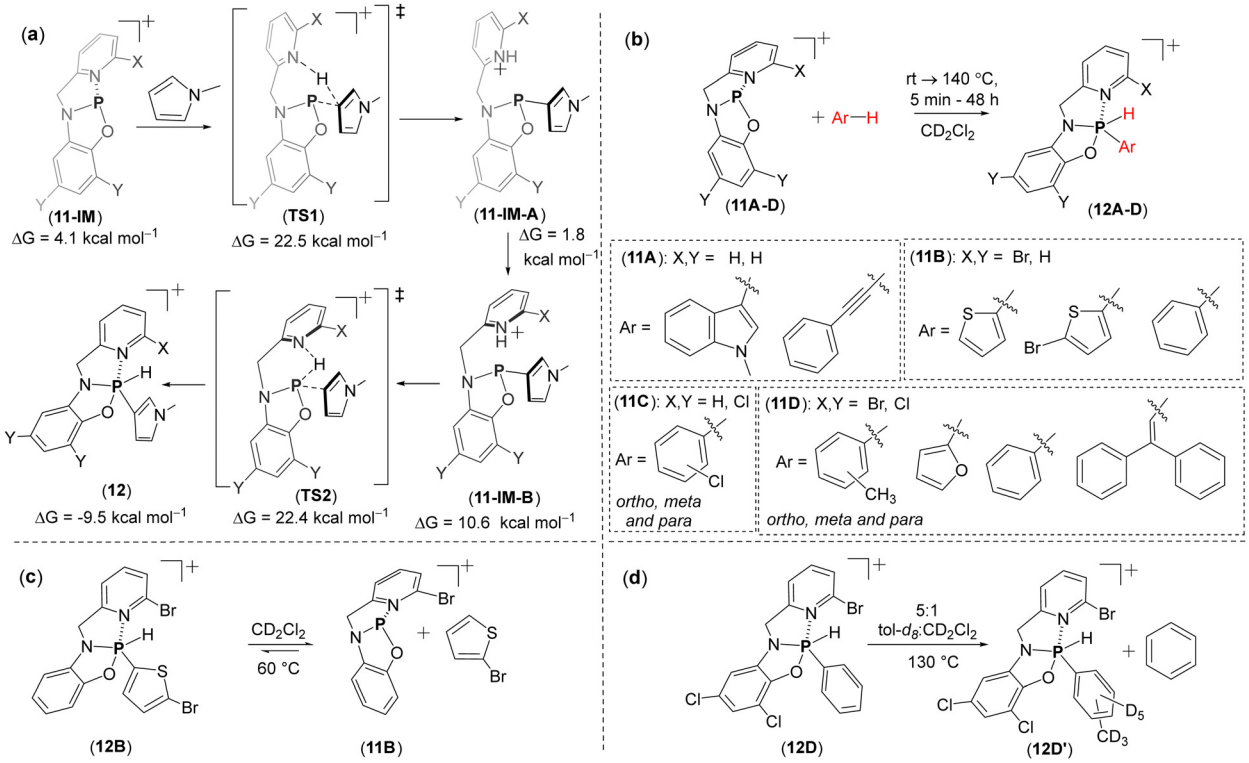

Fig. 7 (a) DFT computed mechanism for C–H bond activation in 1-methylindole by **11**. Synthetic scheme to show: (b) the C–H activation by **11A–D** and (c) and (d) the reductive elimination of C–H bond.

The more electron-poor CSCP species, **11B** and **11D**, could activate less reactive C–H bonds in thiophenes and furanes, leading to OA products (Fig. 7b). Remarkably, **11B** and **11D** also activated the C–H bond in benzene, which overall is very rare in MG chemistry.[98] Similarly, **11D** could activate the C–H bonds in toluene at *ortho*, *meta*, and *para* positions as well as the C–H bond in alkene (in 1,1-diphenylethylene) (Fig. 7b). **11C** was capable of activating the C–H bond in chlorobenzene affording isomeric mixture of the C–H activated products (Fig. 7b).

Most importantly, the OA products herein also undergo reductive elimination and regeneration of the P^{III} species. For example, heating the OA product of **12B** at 60 °C after 1 day leads the regeneration **11B** (71%) and bromothiophene (Fig. 7c). This strategy could be effectively utilized for exchange reactions with other C–H bond-containing arenes. For example, the OA products of **11B** or **11D** with methylthiophene in the presence of 1-methylindole, when kept at rt for one day, yield a more stable indole addition product, with the elimination of methylthiophene. Similarly, the OA product **12D** formed from the reaction of benzene with **11D**, in the presence of toluene-d_8, leads to the formation of the OA product with toluene-d_8, while benzene undergoes reductive elimination (Fig. 7d).

Notably, electrophilic, two-coordinated phosphenium ions can also insert P^{III} centres into the C–H bonds, though their reactivity is generally limited to the activated C–H bonds in metallocenes, xanthene, and cycloheptatriene.[78,99,100] This study emphasized the role of structural constraints in cationic P^{III} species, which enabled the activation of more challenging C–H bonds in a broader range of arenes. Importantly, the reversible RE observed in these reactions suggests promising applications in catalysis.

Recently, Greb and co-workers introduced phosphanylphosphenium **13**, which is a modified version of **11**, where the pyridine-based donor is replaced by a phosphine unit.[85] The central P-centre in **13** is distorted from the C_{3v} symmetry with the bond angles around it ∠P–P–O = 104°, ∠P–P–N = 87° and ∠O–P–N = 94° (in SCXRD) (Fig. 8a). Greb and co-workers show that the structural constraints at the P–P bond in **13** enable it to efficiently engage in the phosphinophosphination (addition of two phosphines to the unsaturated C═X bonds) of various non-activated π-bonded substrates, such as alkynes, alkenes, aldehydes, and ketones (Fig. 8b).

In 2022, Dobrovetsky and co-workers reported CSCP species **17** in which the P centre is incorporated in an *NNN*-type scaffold with anionic pyrrole ''arms'' and a central pyridinyl donor.[86] **17** was synthesized through the chlorophosphine precursor (**17-Cl**) *via* the double deprotonation of the bis(pyrrolyl)pyridine ligand (**17-LH_2**) (Fig. 9a). Reacting **17-Cl** with AgOTf or $[Et_3Si(C_6H_4F_2)][B(C_6F_5)_4]$ led to the facile formation of the corresponding cationic P^{III} species **17** (Fig. 9a).

The SCXRD structure of **17** clearly shows a strong deviation from a local C_{3v} symmetry that could be easily concluded by different bond angles around the P-centre: ∠N_1–P–N_2 = 123°, ∠N_1–P–N_3 and ∠N_2–P–N_3 = 85° (Fig. 9a). Notably, **17** attributes a shorter bond between the pyridine nitrogen and phosphorus atoms (N_3–P 1.752(3)Å) than that of nitrogen of pyrrole ring and phosphorus atom (N_1–P 1.781(2), and N_2–P 1.786(3) Å).

17 rapidly activates O–H and N–H bonds in MeOH and Et_2NH, leading to the formation of LA products as *syn* and *anti*-isomers (Fig. 9b). **17** does not react with dihydrogen, however, it does react with H_3NBH_3 (1 equiv.) producing LA product (**19-H_2**) with isomeric forms (Fig. 9c). Interestingly, **17** reacted with 3 equiv. of H_3NBH_3, producing formally a phosphinidene (P^I product) (**19-(BH_3)$_2$**) in which the P center is coordinated to two BH_3 molecules (Fig. 9c). This P^I species likely forms *via* the addition of BH_3 to the P-centre in an intermediate (**19-BH_3**), which can also be independently synthesized by reacting **17** with 2 equiv. H_3NBH_3, with a concomitant liberation of $[NH_4]^+$.

Interestingly, [**17**][OTf] reacts rapidly with Et_3SiH, *via* a different reaction route compared to its reactions with MeOH, Et_2NH, and H_3NBH_3 that involves the participation of the TfO^-

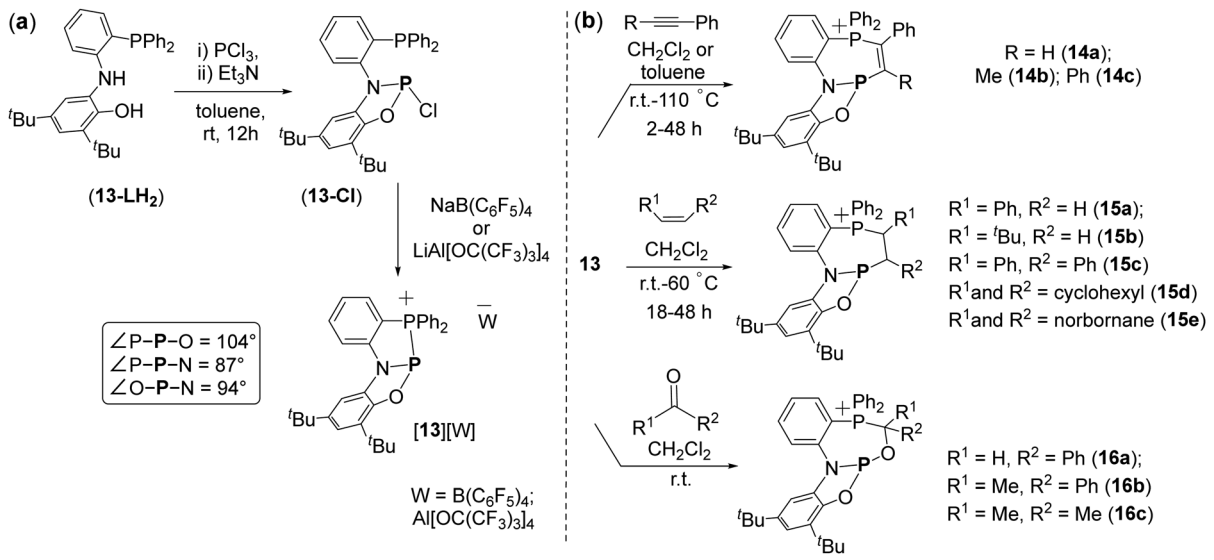

Fig. 8 (a) Synthetic scheme for the synthesis of [**13**][W]; (b) phosphinophosphination of alkynes, olefins, and carbonyls with **13**.

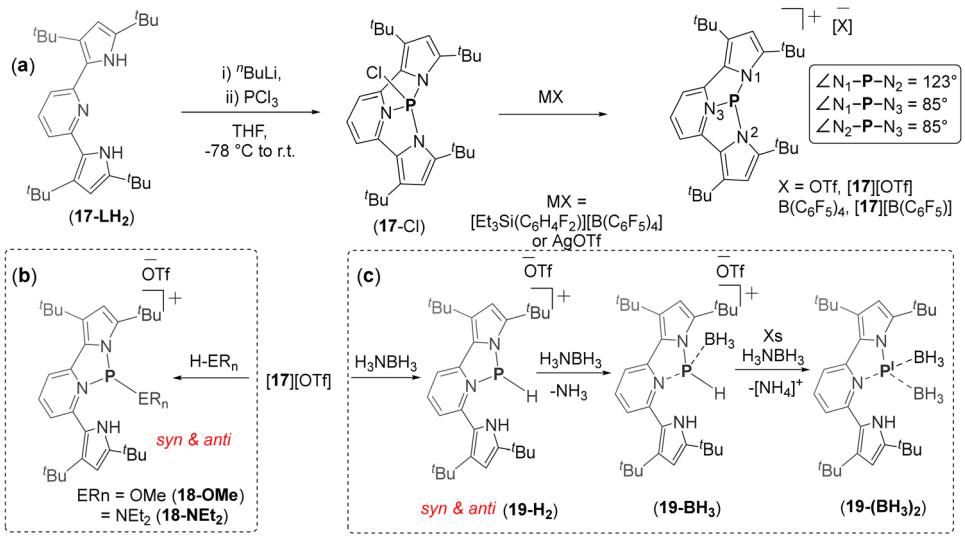

Fig. 9 (a) Synthetic scheme for the synthesis of [**17**][OTf] and [**17**][$B(C_6F_5)_4$]; (b) activation of O–H, N–H bonds and (c) H_3NBH_3 by [**17**][OTf].

anion (Fig. 10a). The reaction proceeds *via* the formation of a hydro-phosphine (**20-H**) and Et_3SiOTf, ultimately resulting in a complex mixture of unidentified products. The Lewis acidic nature of **17** and the non-innocent behaviour of the TfO^- anion likely contribute to this unusual reactivity. Confirmation of this mechanism comes from the reaction of **20-H** (obtained from **17-Cl** and DIBAL-H) with Me_3SiOTf, which shows a similar ^{31}P NMR pattern to the activation of Et_3SiH by [**17**][OTf].

Due to the weaker coordinating nature of the $(C_6F_5)_4B^-$ anion compared to TfO^- anion, the activation of Et_3Si–H bond by [**17**][$B(C_6F_5)_4$] leads to the rapid formation of **21** *via* an unprecedented OA-type reaction of the Si–H bond to the P^{III} center of **17** (Fig. 10a). The formation of this OA product is clearly indicated by the corresponding doublets in the ^1H NMR (9.56 ppm) and ^{31}P NMR (−88.7 ppm), with a similar coupling constant (J = 577 Hz). Notably, **21** was unstable, leading to a complex ^{31}P NMR spectrum that displays a mixture of unidentified products similar to the one obtained from the reaction of [**17**][OTf] with Et_3SiH. Similar ^{31}P NMR spectrum was observed when **20-H** was reacted with [$Et_3Si(C_6H_4F_2)$][$B(C_6F_5)_4$].

DFT computation showed that prior to the activation of the E–H bonds (E = N, O Si) there is an adduct formation between the substrate and **17**. In the case of MeO–H bond activation, first the P–O type adduct is formed (**17-O(H)Me**) with the loss of the symmetry of the P-center supporting *NNN*-ligand (P–N_1: 1.83 Å; P–N_2: 1.95 Å; P–N_3: 1.78 Å). These computations clearly show how **17-O(H)Me** consequently leads to LA product **18-OMe** by proton transfer to the N_2 atom of the ligand (Fig. 10b). In contrast, the adduct **17-H-SiEt$_3$** that is formed prior the OA product **21** has symmetrical *NNN*-ligand around P atom with

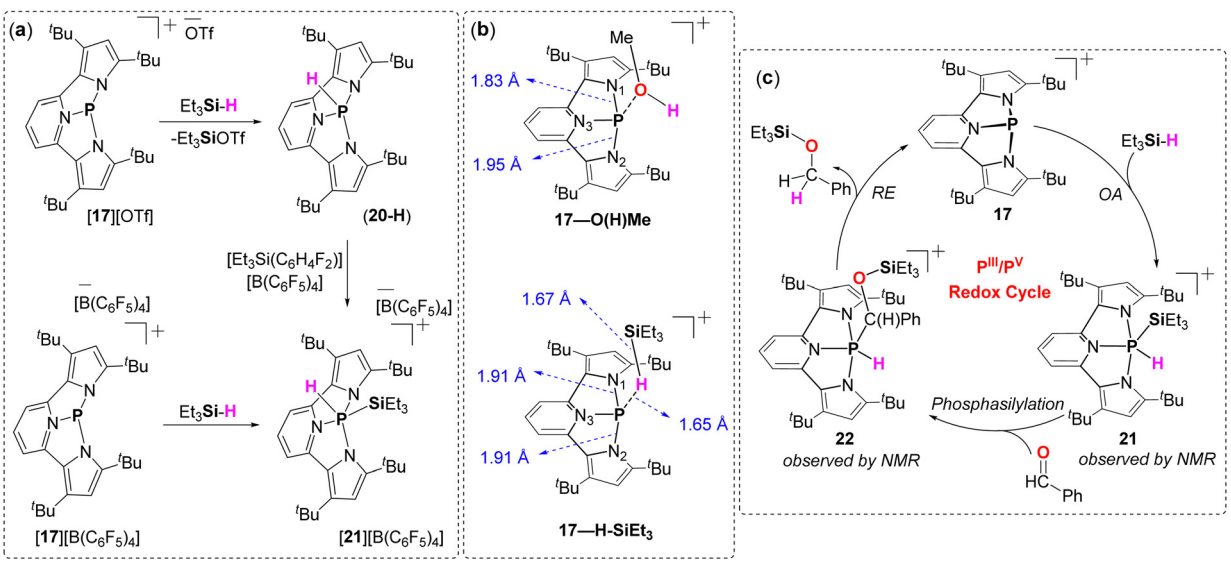

Fig. 10 (a) Si–H bond activation by [**17**][OTf] and [**17**][$B(C_6F_5)_4$]; (b) DFT optimized structure of **17-O(H)Me**, **17-H-SiEt$_3$** and their bond lengths around P atom; (c) hydrosilylation reaction catalyzed by [**17**][$B(C_6F_5)_4$].

slightly elongated P–N_1 (1.91 Å) and P–N_2 (1.91 Å) bonds and a shorter P–N_3 (1.79 Å) bond (Fig. 10b). In addition, longer P–H (1.65 Å) and Si–H (1.67 Å) bonds in **17-H-SiEt$_3$** compared to the P–H bond in **20-H** (1.36 Å), and calculated Et_3Si–H bond (1.50 Å), further support the weakening of the Si–H bond in **17-H-SiEt$_3$** that eventually lead to OA type reaction. Eventually, in **17-H-SiEt$_3$** the bulky Et_3Si-group is positioned far from the pyrrole's basic nitrogen, preferring to bind to the less sterically encumbered lone-pair at the P-center. In contrast, in MeOH and Et_2NH activation, the larger MeO- and Et_2N-groups bind to P-center, while the pyrrole abstracts a proton, avoiding steric congestion (Fig. 10b).

The most compelling feature of this work is the catalytic hydrosilylation of C=O bonds in benzaldehyde, mediated by **17**, which emulates the behaviour of the TM complexes by following a similar catalytic cycle (Fig. 10c). In this process, benzaldehyde reacts with Et_3SiH in the presence of 5 mol% of [**17**][$B(C_6F_5)_4$], resulting in the formation of the corresponding silyl ether, Et_3SiO–$C(H_2)$Ph, after 12 hours at 50 °C. The stepwise progress of this reaction revealed first formation of an OA product **21** ($^{31}P(\delta)$ = −88.73 ppm), followed by a phosphasilylation producing the migratory insertion intermediate **22** ($^{31}P(\delta)$ = −74.54 ppm; $^{1}J_{P-H}$ = 648 Hz) and finally, a reductive elimination type reaction from P^V centre in **22** producing Et_3SiO–$C(H_2)$Ph and regeneration of the active catalyst **17** (Fig. 10c).

Carbone-based carbodiphosphorane (CDP)[101] scaffolds are increasingly being employed to construct complexes with MG elements.[14–16,102–104] Specifically, the hexaphenyl-carbodiphosphoranyl-based *CCC* pincer-type ligand (**23-LH$_2$**) is benefited from a strong donor carbon center and the facile deprotonation of the phenyl rings, which together impart an excellent ability to obtain dianionic, tridentate *CCC* pincer-type ligand that can be used to structurally constrain MG centers. Recent examples highlight the use of **23-LH$_2$** to incorporate neutral beryllium species, as well as cationic antimony and bismuth species.[14–16,102–104] In the case of phosphorus, deprotonation of **23-LH$_2$**, followed by reaction with PCl_3, results in the production of a cationic SC P^{III} species, [**24**][Cl].[87] An anion exchange with K[PF_6] leads to of [**24**][PF_6] (Fig. 11a).

A significant distortion around the P center is induced by the *CCC* framework in **24**, resulting in wider ∠C_1–P–C_2 (106°) and narrower ∠C_1–P–C_3 (95°) and ∠C_2–P–C_3 (96°) bond angles (Fig. 10a). However, the degree of distortion in **24** is less pronounced than that observed in previously reported SCP species (**XIII-XIV**) featuring the *CCC* framework (Fig. 3d).

Notably, **24** is inert toward Et_2NH, MeOH, and Et_3SiH, however, it reacts with electron-poor fluoroarenes at elevated temperatures (80–120 °C) readily leading to the formation of the OA products of the C–F bond to the P^{III} centre in **24** (Fig. 11b). For instance, the reaction of [**24**][PF_6] with pentafluoropyridine in 1,2-difluorobenzene (*o*DFB) for 3 h at 80 °C clearly demonstrates the formation of the OA product [**25**][PF_6], as indicated by a doublet of triplets ($^{1}J_{PF}$ = 666 Hz; $^{2}J_{PP}$ = 52 Hz) at δ = −48.87 ppm in ^{31}P NMR spectrum with a complementary doublet ($^{1}J_{PF}$ = 666 Hz) at δ = 1.92 ppm in ^{19}F NMR (Fig. 12).

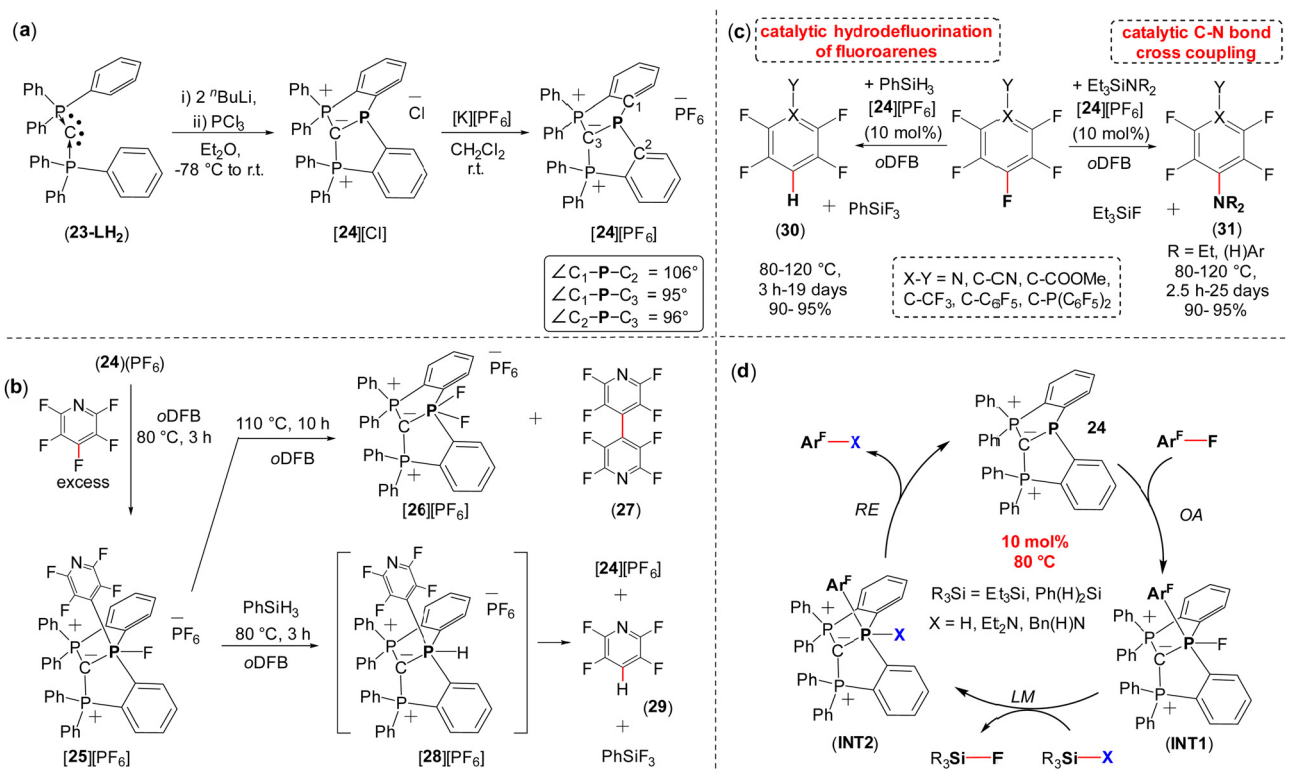

Fig. 11 Synthetic scheme for (a) the synthesis of [**24**][PF_6]; (b) the formation of [**25**][PF_6] by the activation of C–F bond and its further reactions; (c) the hydrodefluorination and C–N bond forming cross-coupling reactions catalyzed by **24**; (d) and the scheme for proposed computational mechanism.

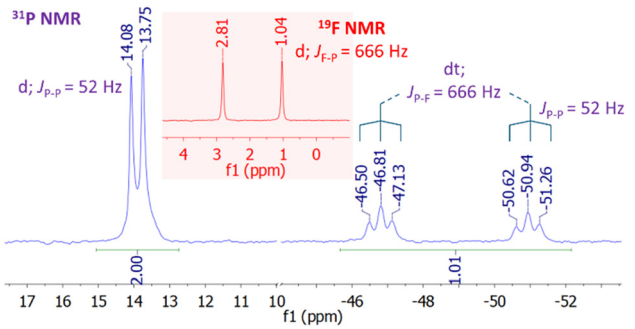

Fig. 12 ^{31}P and ^{19}F NMR spectra showing the formation of the OA product [**25**][PF_6].

Interestingly, heating [**25**][PF_6] to 110 °C for 10 hours results in the formation of a difluoro-species, [**26**][PF_6], likely being mediated through a disproportionation mechanism involving a series of ligand exchange reactions followed by the elimination of perfluoro-4,4′-bipyridine (**27**) (Fig. 11b). In contrast, heating [**25**][PF_6] in the presence of $PhSiH_3$ at 80 °C for 3 h directly leads to the regeneration of [**24**][PF_6], $PhSiF_3$ and the product of hydrodefluorination (**29**). This transformation likely proceeds through hydrophosphorane intermediate [**28**][PF_6] followed by a rapid RE of the C–H bond from the P-centre (Fig. 11b). Notably, similar reactivity was observed for the reaction with neutral SCP (**V**), but this reaction led to the hydrodefluorination products *via* a stable hydrophosphorane intermediate in the reaction with DIBAL-H.[43]

In contrast to **V**, the reactivity of **24** with fluoroarenes, coupled with its inertness toward hydrosilanes allowed the catalytic hydrodefluorination of fluoroarenes using $PhSiH_3$ and 10 mol% [**24**][PF_6] (Fig. 11c). Various fluoroarenes with different functional groups (F_3C-, NC-, MeOC(O)-) could be catalytically hydrodefluorinated in good to excellent yields (90–95%). Importantly, the catalytic hydrodefluorination of fluoroarenes by **24** proceeds *via* a metallomimetic P^{III}/P^{V} redox cycle.

Remarkably, the reactivity of **24** was also successfully extended to the catalytic C–N bond-forming cross-coupling reaction products (Fig. 11c). The substrate scope includes the reaction of various fluoroarenes with $Et_3Si–NR_2$ (R = Et, (H)Ar) in presence of 10 mol% of [**24**][PF_6] in *o*DFB, at elevated temperatures (80–120 °C).

Both experimental and computational studies suggest that the mechanisms of both hydrodefluorination and C–N bond forming cross-coupling proceed in a metallomimetic fashion through the OA → LM → RE steps (Fig. 11d). Notably, a similar catalytic transformation was later reported with simple phosphines, however, the mechanism was distinctively different.[7]

Very recently, the Dobrovetsky group reported another example of pyridine based CSCP, [**34**][$B(C_6F_5)_4$], using a *CNC*-type of pincer type ligand (**32-LH$_2$**) (Fig. 13a).[88] The *CNC*-type ligand consists of a pyridine ring attached to two *o*-carborane units.[105] While the nitrogen atom of the pyridine ring stabilizes the cationic P center, the electron-withdrawing nature of the carborane units enhances the Lewis acidity of the P centre. Additionally, the *o*-carboranyl units are easily deprotonated at the C–H position, and their rigid structure imposes additional constraint at the P centre. Thus deprotonation of **32-LH$_2$**, followed by reaction with PCl_3 affords a chlorophosphine **33-Cl** (Fig. 13a). Chloride abstraction from **33-Cl** using [$Et_3Si(C_7H_8)$]-[$B(C_6F_5)_4$] results in the formation of the cationic P^{III} species, [**34**][$B(C_6F_5)_4$].

34 exhibited a highly distorted geometry around the P center (∠C_1–P–C_2 = 124°, ∠C_1–P–N and ∠C_2–P–N = 87°) (Fig. 13a). In contrast to the aforementioned CSCPs, a significant difference in the reactivity was observed for **34**, as evidenced by its ability to activate dihydrogen (H_2) at a single P^{III} centre, resulting in the formation of the formal OA product **34-H$_2$** (Fig. 13b). It is important to note that while the activation of H_2 by OA-type process has been observed at several low-valent MG centres, such as carbenes,[3,45,106] borylenes,[3,107–109] and their heavier analogues,[110–115] the activation of H_2 at a single P^{III} centre was never reported, which makes the reactivity of H_2 with **34** unprecedented and provides new insight into the influence of SC and cationic character of this center. It is also important to note that the activation of H_2 between either two phosphorus centers or between phosphorus and other MG center was reported with Frustrated Lewis acid–base pairs being the prime examples of this type of reactivity.

Importantly, all attempts to liberate H_2 from [**34-H$_2$**]-[$B(C_6F_5)_4$] failed and the reductive elimination did not occur, which indicated that the H_2 activation by **34** is irreversible. Interestingly, when [**34-H$_2$**][$B(C_6F_5)_4$] was dissolved in deuterated aromatics (C_6D_6, tol-d_8) at 50 °C, an exchange reaction between H and D atoms occurred at the aromatic ring over the course of 3 h, leading to [**34-D$_2$**][$B(C_6F_5)_4$] and C_6H_6 (or $C_6H_5CD_3$) (Fig. 13b). Conversely, a similar behaviour was observed for [**34-D$_2$**][$B(C_6F_5)_4$] in the presence of toluene leading to the formation of [**34-H$_2$**][$B(C_6F_5)_4$] and $C_6D_5CH_3$.

The DFT computed mechanism of H_2 activation by **34** reveals that this process is electrophilically driven, with the H–H σ-bond approaching the cationic P-centre from the direction of the LUMO in the asynchronous transition state (TS) (Fig. 13c–e). This is followed by the interaction of the HOMO of the P-centre with the LUMO (σ*) of the H–H bond (Fig. 13c–e).

As mentioned previously, despite the ability of several low-valent MG compounds such as carbenes, borylenes, and their heavier analogues to activate the H–H bond by OA, the hydrogenation reaction using these MG species was never reported. In contrast, [**34**][$B(C_6F_5)_4$] could be further used in hydrogenation of various unsaturated C–C bonds and fused aromatic systems (Fig. 13f). Mechanistic and experimental studies of the hydrogenation process suggested that the first step of this process is OA of H_2 to P^{III} centre in **34** producing **34-H$_2$**. Deprotonation of **34-H$_2$** by the doubly-bonded species at next step, produces the corresponding carbocation and **35-H** (Fig. 13g and h). The last step is the hydride abstraction from the **35-H** by the carbocation producing the hydrogenated products and regenerated catalyst (**34**) (Fig. 13g and h). This was supported by a sequential deprotonation and hydride abstraction of **34-H$_2$** by first Et_2O and second Ph_3C^+ (Fig. 13g).

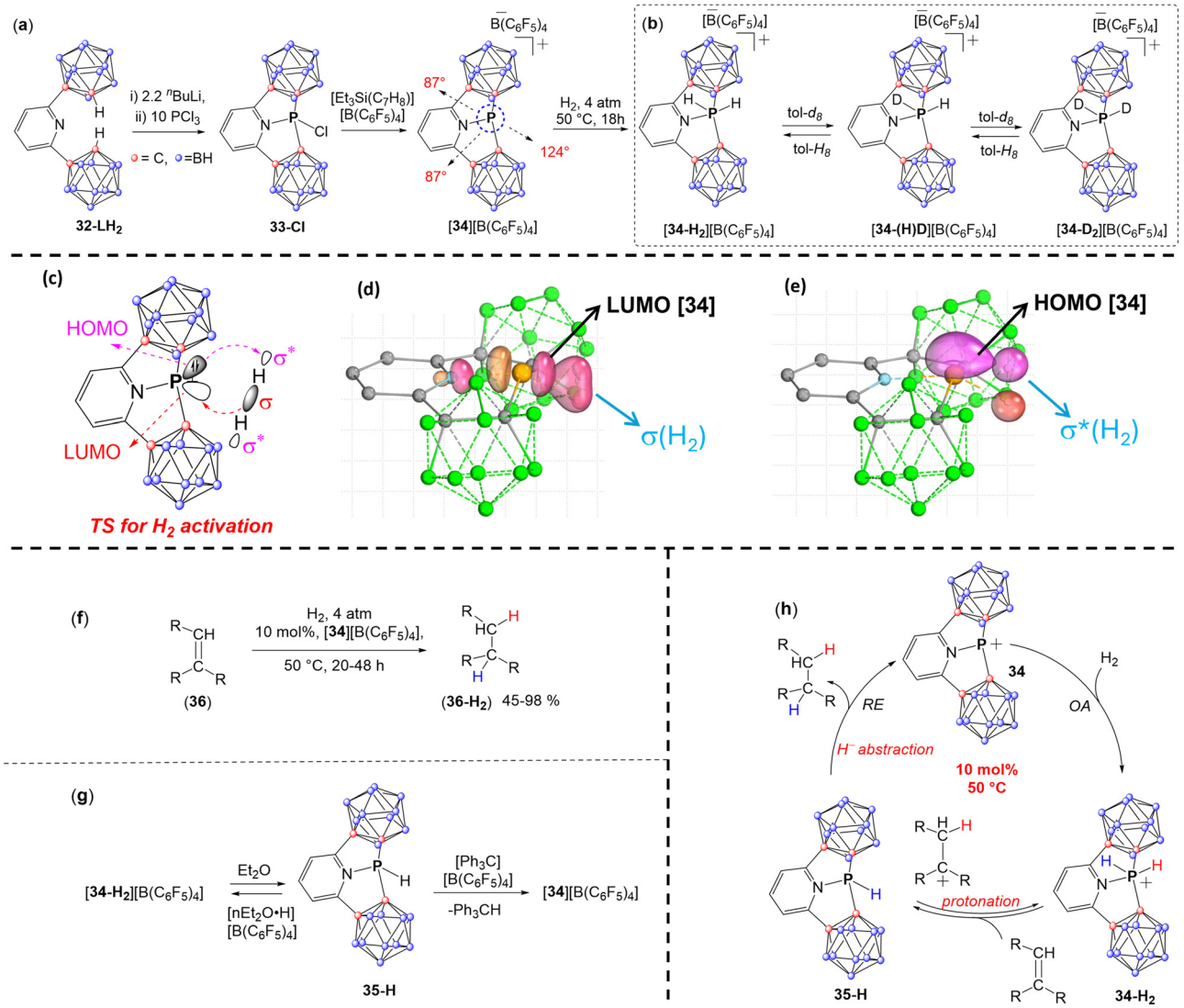

Fig. 13 Synthetic scheme for (a) the synthesis of [**34**][$B(C_6F_5)_4$]; (b) the activation of dihydrogen by [**34**][$B(C_6F_5)_4$] and the exchange reaction between H and D atom between [**34-H$_2$**][$B(C_6F_5)_4$] and toluene-d_8 and *vice-versa*; (c) schematic representation to show electrophilically driven activation of the H–H bond by **34**.; (d) σ-bond of H_2 approaching the P-centre from the direction of the LUMO of **34**; (e) followed by the interaction of the HOMO of the P-centre with the LUMO (σ*) of H_2; (f) [**34**][$B(C_6F_5)_4$] catalyzed hydrogenation reactions of unsaturated C–C species; (g) equilibrium of [**34**][$B(C_6F_5)_4$] with **35-H** and reaction of **35-H** with $[Ph_3C][B(C_6F_5)_4]$; and (h) the proposed catalytic cycle.

3. Conclusions

In this review, we discussed the chemistry of cationic structurally constrained phosphines (CSCPs) and their use in the activation of small molecules and catalysis. While most phosphines do not exhibit significant reactivity toward challenging bonds, the application of the structural constraint (SC) to phosphorus enhances their reactivity and leads to ambiphilic phosphorus centers capable of activating such bonds. Despite significant progress with structurally constrained phosphines, their ability to catalyze reactions remains very limited.

Recently, a new class of SCPs—cationic SCPs (CSCPs)—was designed, in which the combination of SC and cationic charge enables these P-compounds to not only activate challenging bonds but also participate in catalysis. The CSCPs highlighted in this review demonstrated reversible activation of O–H and N–H bonds. They were also shown to activate C–F bonds in fluoroarenes through oxidative addition (OA)-type reactions, enabling catalytic hydrodefluorination and C–N bond-forming cross-coupling reactions with elementary steps reminiscent of TM-based catalytic cycles. Remarkably, these species were capable of activating Si–H, C–H, and H–H bonds through OA-type reactions, and participate in phosphino-phosphination reactions of C=C double bonds. While the activation of C–H bonds has yet to find applications in catalysis, Si–H and H–H bond activations were successfully employed in catalytic hydrosilylation and hydrogenation reactions, mimicking TM-like behavior.

CSCPs have already proven to be promising species for the activation of challenging bonds. However, their full potential

for activating other challenging bonds and their broader applications in catalysis remain to be explored.

Data availability

No primary research results, software or code have been included, and no new data were generated or analysed as part of this review.

Conflicts of interest

There are no conflicts to declare.

Acknowledgements

This work was supported by the Israeli Science Foundation, Grant 195/22, and the Israel Ministry of Science Technology & Space, Grant 01032376. D. B. thanks Raymond & Beverley Sackler for the Postdoctoral fellowship. D. T. thanks the Ariane de Rothschild Women Doctoral scholarship for outstanding female PhD students.

References

1 P. P. Power, *Nature*, 2010, **463**, 171–177.
2 C. Weetman and S. Inoue, *ChemCatChem*, 2018, **10**, 4213–4228.
3 T. Chu and G. I. Nikonov, *Chem. Rev.*, 2018, **118**, 3608–3680.
4 R. L. Melen, *Science*, 2019, **363**, 479–484.
5 C. Xie, A. J. Smaligo, X.-R. Song and O. Kwon, *ACS Cent. Sci.*, 2021, **7**, 536–558.
6 H. Fujimoto, K. Yasui and M. Tobisu, *Bull. Chem. Soc. Jpn.*, 2023, **96**, 872–886.
7 S. Bonfante, C. Lorber, J. M. Lynam, A. Simonneau and J. M. Slattery, *J. Am. Chem. Soc.*, 2024, **146**, 2005–2014.
8 P. Šimon, R. Jambor, A. Růžička and L. Dostál, *Organometallics*, 2013, **32**, 239–248.
9 C. Ganesamoorthy, C. Wölper, L. Dostál and S. Schulz, *J. Organomet. Chem.*, 2017, **845**, 38–43.
10 M. Huang, K. Li, Z. Zhang and J. Zhou, *J. Am. Chem. Soc.*, 2024, **146**, 20432–20438.
11 H. W. Moon and J. Cornella, *ACS Catal.*, 2022, **12**, 1382–1393.
12 M. Mato and J. Cornella, *Angew. Chem., Int. Ed.*, 2024, **63**, e202315046.
13 M. K. Mondal, L. Zhang, Z. Feng, S. Tang, R. Feng, Y. Zhao, G. Tan, H. Ruan and X. Wang, *Angew. Chem., Int. Ed.*, 2019, **58**, 15829–15833.
14 D. Obi, D. A. Dickie, W. Tiznado, G. Frenking, S. Pan and R. J. GilliardJr, *Inorg. Chem.*, 2022, **61**, 19452–19462.
15 A. D. Obi, C.-L. Deng, A. J. Alexis, D. A. Dickie and R. J. Gilliard Jr., *Chem. Commun.*, 2024, **60**, 1880–1883.
16 L. Warring, K. S. Westendorff, M. T. Bennett, K. Nam, B. M. Stewart, D. A. Dickie, C. Paolucci, T. B. Gunnoe and R. J. GilliardJr, *Angew. Chem., Int. Ed.*, 2025, **64**, e202415070.
17 M. B. Kindervater, K. M. Marczenko, U. Werner-Zwanziger and S. S. Chitnis, *Angew. Chem., Int. Ed.*, 2019, **58**, 7850–7855.
18 T. Hynes, J. D. Masuda and S. S. Chitnis, *ChemPlusChem*, 2022, e202200244.
19 K. M. Marczenko, J. A. Zurakowski, M. B. Kindervater, S. Jee, T. Hynes, N. Roberts, S. Park, U. Werner-Zwanziger, M. Lumsden, D. N. Langelaan and S. S. Chitnis, *Chem. – Eur. J.*, 2019, **25**, 16414–16424.
20 S. Kundu, *Chem. – Asian J.*, 2020, **15**, 3209–3224.
21 J. Abbenseth and J. M. Goicoechea, *Chem. Sci.*, 2020, **11**, 9728–9740.
22 J. M. Lipshultz, G. Li and A. T. Radosevich, *J. Am. Chem. Soc.*, 2021, **143**, 1699–1721.
23 A. Maiti, R. Yadav and L. Greb, Structural constraint effects on p-block elements: Recent advances, chapter 8, *Adv. Inorg. Chem.*, 2023, **82**, 261–299.
24 T. J. Hannaha and S. S. Chitnis, *Chem. Soc. Rev.*, 2024, **53**, 764–792.
25 D. Houalla, F. H. Osman, M. Sanchez and R. Wolf, *Tetrahedron Lett.*, 1977, **35**, 3041–3044.
26 R. Wolf, *Pure Appl. Chem.*, 1980, **52**, 1141–1150.
27 C. Bonningue, D. Houalla, M. Sanchez and R. Wolf, *J. Chem. Soc., Perkin Trans. 2*, 1981, 19.
28 C. Bonningue, D. Houalla and R. Wolf, *J. Chem. Soc., Perkin Trans. 2*, 1983, 773–776.
29 R. Contreras, A. Murillo, G. Uribe and A. Klaébé, *Heterocycles*, 1985, **23**, 2187–2192.
30 A. Murillo, L. M. Chiquete, P. Joseph-Nathan and R. Contreras, *Phosphorus, Sulfur Silicon Relat. Elem.*, 1990, **53**, 87–101.
31 R. Contreras, A. Murillo and P. Joseph-Nathan, *Phosphorus, Sulfur Silicon Relat. Elem.*, 1990, **47**, 215–224.
32 C. Camacho-Camacho, F. J. Martínez-Martínez, M. De Jesús Rosales-Hoz and R. Contreras, *Phosphorus, Sulfur Silicon Relat. Elem.*, 1994, **91**, 189–203.
33 G. Baccolini, E. Mezzina, P. E. Todesco and E. Foresti, *J. Chem. Soc., Chem. Commun.*, 1988, 304–305.
34 G. Baccolini, E. Mezzina and P. E. Todesco, *J. Chem. Soc., Perkin Trans. 1*, 1988, 3281–3283.
35 G. Baccolini, C. A. Mosticchio, E. Mezzina, C. Rizzoli and P. Sgarabotto, *Heteroat. Chem.*, 1993, **4**, 319–322.
36 S. A. Culley and A. J. Arduengo, *J. Am. Chem. Soc.*, 1984, **106**, 1164–1165.
37 A. J. Arduengo, C. A. Stewart, F. Davidson, D. A. Dixon, J. Y. Becker, S. A. Culley and M. B. Mizen, *J. Am. Chem. Soc.*, 1987, **109**, 627–647.
38 N. L. Dunn, M. Ha and A. T. Radosevich, *J. Am. Chem. Soc.*, 2012, **134**, 11330–11333.
39 S. M. McCarthy, Y.-C. Lin, D. Devarajan, J. W. Chang, H. P. Yennawar, R. M. Rioux, D. H. Ess and A. T. Radosevich, *J. Am. Chem. Soc.*, 2014, **136**, 4640–4650.
40 W. Zhao, S. M. McCarthy, T. Yi Lai, H. P. Yennawar and A. T. Radosevich, *J. Am. Chem. Soc.*, 2014, **136**, 17634–17644.
41 H. W. Moon, A. Maity and A. T. Radosevich, *Organometallics*, 2021, **40**, 2785–2791.
42 Y.-C. Lin, E. Hatzakis, S. M. McCarthy, K. D. Reichl, T.-Y. Lai, H. P. Yennawar and A. T. Radosevich, *J. Am. Chem. Soc.*, 2017, **139**, 6008–6016.
43 S. Lim and A. T. Radosevich, *J. Am. Chem. Soc.*, 2020, **142**, 16188–16193.
44 (*a*) O. Elishav, B. M. Lis, E. M. Miller, D. J. Arent, A. Valera-Medina, A. G. Dana, G. E. Shter and G. S. Grader, *Chem. Rev.*, 2020, **120**, 5352–5436; (*b*) S. Streiff and F. Jérôme, *Chem. Soc. Rev.*, 2021, **50**, 1512–1521; (*c*) J. Zhao, A. S. Goldman and J. F. Hartwig, *Science*, 2005, **307**, 1080–1082; (*d*) E. Morgan, D. F. MacLean, R. McDonald and L. Turculet, *J. Am. Chem. Soc.*, 2009, **131**, 14234–14236.
45 G. D. Frey, V. Lavallo, B. Donnadieu, W. W. Schoeller and G. Bertrand, *Science*, 2007, **316**, 439–441.
46 Z. Zhu, X. Wang, Y. Peng, H. Lei, J. C. Fettinger, E. Rivard and P. P. Power, *Angew. Chem., Int. Ed.*, 2009, **48**, 2031–2034.
47 J. A. B. Abdalla, I. M. Riddlestone, R. Tirfoin and S. Aldridge, *Angew. Chem., Int. Ed.*, 2015, **54**, 5098–5102.
48 A. Jana, C. Schulzke and H. W. Roesky, *J. Am. Chem. Soc.*, 2009, **131**, 4600–4601.
49 Y. Peng, B. D. Ellis, X. Wang and P. P. Power, *J. Am. Chem. Soc.*, 2008, **130**, 12268–12269.
50 A. V. Protchenko, J. I. Bates, L. M. A. Saleh, M. P. Blake, A. D. Schwarz, E. L. Kolychev, A. L. Thompson, C. Jones, P. Mountford and S. Aldridge, *J. Am. Chem. Soc.*, 2016, **138**, 4555–4564.
51 D. Wendel, T. Szilvási, D. Henschel, P. J. Altmann, C. Jandl, S. Inoue and B. Rieger, *Angew. Chem., Int. Ed.*, 2018, **57**, 14575–14579.
52 F. Dankert, J.-E. Siewert, P. Gupta, F. Weigend and C. Hering-Junghans, *Angew. Chem., Int. Ed.*, 2022, **61**, e202207064.
53 A. L. Humphries, G. A. Tellier, M. D. Smith, A. R. Chianese and D. V. Peryshkov, *J. Am. Chem. Soc.*, 2024, **146**, 33159–33168.
54 J. Cui, Y. Li, R. Ganguly, A. Inthirarajah, H. Hirao and R. Kinjo, *J. Am. Chem. Soc.*, 2014, **136**, 16764–16767.
55 T. P. Robinson, D. M. De Rosa, S. Aldridge and J. M. Goicoechea, *Angew. Chem., Int. Ed.*, 2015, **54**, 13758–13763.

56 J. Abbenseth, O. P. E. Townrow and J. M. Goicoechea, *Angew. Chem., Int. Ed.*, 2021, **60**, 23625–23629.
57 N. Beims, T. Greven, M. Schmidtmann and J. I. van der Vlugt, *Chem. – Eur. J.*, 2023, **29**, e202302463.
58 A. Tanushi and A. T. Radosevich, *J. Am. Chem. Soc.*, 2018, **140**, 8114–8118.
59 A. J. King, J. Abbenseth and J. M. Goicoechea, *Chem. – Eur. J.*, 2023, **29**(1–12), e202300818.
60 A. Hentschel, A. Brand, P. Wegener and W. Uhl, *Angew. Chem., Int. Ed.*, 2018, **57**, 832–835.
61 A. Brand, A. Hentschel, A. Hepp and W. Uhl, *Eur. J. Inorg. Chem.*, 2020, 361–369.
62 K. Dimroth and P. Hoffmann, *Angew. Chem., Int. Ed. Engl.*, 1964, **3**, 384.
63 D. Gudat, *Acc. Chem. Res.*, 2010, **43**, 1307–1316.
64 D. Gudat, *Dalton Trans.*, 2016, **45**, 5896–5907.
65 D. Gudat, *Eur. J. Inorg. Chem.*, 1998, 1087–1094.
66 D. Gudat, A. Haghverdi, H. Hupfer and M. Nieger, *Chem. – Eur. J.*, 2000, **6**, 3414–3425.
67 H. M. Tuononen, R. Roesler, J. L. Dutton and P. J. Ragogna, *Inorg. Chem.*, 2007, **46**, 10693–10706.
68 A. L. Brazeau, C. A. Caputo, C. D. Martin, N. D. Jones and P. J. Ragogna, *Dalton Trans.*, 2010, **39**, 11069–11073.
69 D. Gudat, *Coord. Chem. Rev.*, 1997, **163**, 71–106.
70 H. Nakazawa, *J. Organomet. Chem.*, 2000, **611**, 349–363.
71 L. Rosenberg, *Coord. Chem. Rev.*, 2012, **256**, 606–626.
72 N. Burford, D. E. Herbert, P. J. Ragogna, R. McDonald and M. J. Ferguson, *J. Am. Chem. Soc.*, 2004, **126**, 17067–17073.
73 C. A. Caputo, M. C. Jennings, H. M. Tuononen and N. D. Jones, *Organometallics*, 2009, **28**, 990–1000.
74 T. W. Hudnall, J. P. Moerdyka and C. W. Bielawski, *Chem. Commun.*, 2010, **46**, 4288–4290.
75 U. Siemeling, C. Färber, C. Bruhn, M. Leibold, D. Selent, W. Baumann, M. von Hopffgarten, C. Goedeckec and G. Frenking, *Chem. Sci.*, 2010, **1**, 697–704.
76 C. A. Caputo, J. T. Price, M. C. Jennings, R. McDonald and N. D. Jones, *Dalton Trans.*, 2008, 3461–3469.
77 C. M. Feil, F. Goerigk, Y. Stöckl, M. Nieger and D. Gudat, *Dalton Trans.*, 2025, **54**, 1806–1814.
78 N. Đorđević, R. Ganguly, M. Petković and D. Vidović, *Inorg. Chem.*, 2017, **56**, 14671–14681.
79 M. Q. Y. Tay, Y. Lu, R. Ganguly and D. Vidović, *Chem. – Eur. J.*, 2014, **20**, 6628–6631.
80 (*a*) D. Bawari, S. Volodarsky, Y. Ginzburg, K. Jaiswal, P. Joshi and R. Dobrovetsky, *Chem. Commun.*, 2022, **58**, 12176–12179; (*b*) P. Wang, Q. Zhu, Y. Wang, G. Zeng, J. Zhu and C. Zhu, *Chin. Chem. Lett.*, 2021, **32**, 1432–1436.
81 X. Tan and H. Wang, *Chem. Soc. Rev.*, 2022, **51**, 2583–2600.
82 S. Volodarsky and R. Dobrovetsky, *Chem. Commun.*, 2018, **54**, 6931–6934.
83 D. Bawari, I. Malahov and R. Dobrovetsky, *Angew. Chem., Int. Ed.*, 2024, (7 of 9), e202419772.
84 D. Roth, A. T. Radosevich and L. Greb, *J. Am. Chem. Soc.*, 2023, **145**, 24184–24190.
85 L. You, D. Roth and L. Greb, *Chem. Sci.*, 2025, **16**, 1716–1721.
86 S. Volodarsky, D. Bawari and R. Dobrovetsky, *Angew. Chem., Int. Ed.*, 2022, **61**(1–8), e202208401.
87 K. Chulsky, I. Malahov, D. Bawari and R. Dobrovetsky, *J. Am. Chem. Soc.*, 2023, **145**, 3786–3794.
88 D. Bawari, D. Toami, K. Jaiswal and R. Dobrovetsky, *Nat. Chem.*, 2024, **16**, 1261–1266.
89 T. P. Robinson, S.-K. Lo, D. De Rosa, S. Aldridge and J. M. Goicoechea, *Chem. – Eur. J.*, 2016, **22**, 15712–15724.
90 M. J. Panzner, C. A. Tessier and W. J. Youngs, Pincer complexes of N-heterocyclic carbenes. *Potential uses as pharmaceuticals, The Chemistry of Pincer Compounds*, ed. D. Morales-Morales and C. M. Jensen, Elsevier, Amsterdam, The Netherlands, 2007, 139–150.
91 D. Zhang and G. Zi, *Chem. Soc. Rev.*, 2015, **44**, 1898–1921.
92 R. Taakili and Y. Canac, *Molecules*, 2020, **25**, 2231.
93 I. Jain and P. Malik, *Eur. Polym. J.*, 2021, **150**, 110412.
94 N. Matsumura, J. Kawano, N. Fukunishi and H. Inoue, *J. Am. Chem. Soc.*, 1995, **117**, 3623–3624.
95 C. Romain, C. Fliedel, S. Bellemin-Laponnaz and S. Dagorne, *Organometallics*, 2014, **33**, 5730–5739.
96 J. M. Farrell and D. W. Stephan, *Angew. Chem., Int. Ed.*, 2015, **54**, 5214–5217.
97 D. Bawari, S. Volodarsky, Y. Ginzburg, K. Jaiswal, P. Joshi and R. Dobrovetsky, *Dalton Trans.*, 2021, **50**, 16478–16482.
98 J. Hicks, P. Vasko, J. M. Goicoechea and S. Aldridge, *Nature*, 2018, **557**, 92–95.
99 A. H. Cowley, R. A. Kemp and C. A. Stewart, *J. Am. Chem. Soc.*, 1982, **104**, 3239–3240.
100 A. Jayaraman and B. T. Sterenberg, *Organometallics*, 2016, **35**, 2367–2377.
101 F. Ramirez, B. Hansen, N. B. Desai and N. McKelvie, *J. Am. Chem. Soc.*, 1961, **83**, 3539–3540.
102 M. R. Buchner, S. Pan, C. Poggel, N. Spang, M. Müller, G. Frenking and J. Sundermeyer, *Organometallics*, 2020, **39**, 3224–3231.
103 P. Dabringhaus, A. Molino and R. J. GilliardJr, *J. Am. Chem. Soc.*, 2024, **146**, 27186–27195.
104 Z. Liu, Z. Wang, H. Mu, Y. Zhou, J. Zhou and Z. Dong, *Nat. Commun.*, 2024, **15**, 9849.
105 K. P. Anderson, H. A. Mills, C. Mao, K. O. Kirlikovali, J. C. Axtell, A. L. Rheingold and A. M. Spokoyny, *Tetrahedron*, 2019, **75**, 187–191.
106 D. Martin, M. Soleilhavoup and G. Bertrand, *Chem. Sci.*, 2011, **2**, 389–399.
107 F. Dahcheh, D. Martin, D. W. Stephan and G. Bertrand, *Angew. Chem., Int. Ed.*, 2014, **53**, 13159–13163.
108 M. Soleilhavoup and G. Bertrand, *Angew. Chem., Int. Ed.*, 2017, **56**, 10282–10292.
109 M.-A. Légaré, C. Pranckevicius and H. Braunschweig, *Chem. Rev.*, 2019, **119**, 823–8261.
110 J. Hicks, P. Vasko, J. M. Goicoechea and S. Aldridge, *Nature*, 2018, **557**, 92–95.
111 J. Hicks, P. Vasko, J. M. Goicoechea and S. Aldridge, *Angew. Chem., Int. Ed.*, 2021, **60**, 1702–1713.
112 A. V. Protchenko, K. H. Birjkumar, D. Dange, A. D. Schwarz, D. Vidovic, C. Jones, N. Kaltsoyannis, P. Mountford and S. Aldridge, *J. Am. Chem. Soc.*, 2012, **134**, 6500–6503.
113 G. H. Spikes, J. C. Fettinger and P. P. Power, *J. Am. Chem. Soc.*, 2005, **127**, 12232–12233.
114 Y. Peng, B. D. Ellis, X. Wang and P. P. Power, *J. Am. Chem. Soc.*, 2008, **130**, 12268–12269.
115 Y. Pang, M. Leutzsch, N. Nöthling and J. Cornella, *Angew. Chem., Int. Ed.*, 2023, **62**, e202302071.

